



1
2
3
4
5
6
7
8
9
10
11
12
13
14
15
16
17
18
19
20
21
22

**Effect of tropical cyclones on the Stratosphere-Troposphere Exchange
observed using satellite observations over north Indian Ocean**

M. Venkat Ratnam^{1*}, S. Ravindra Babu², S.S. Das³, GhouseBasha⁴, B.V. Krishnamurthy⁵
and B.Venkateswararao²

¹National Atmospheric Research Laboratory (NARL), Gadanki, India.

²Jawaharlal Nehru Technological University, Hyderabad, India.

³Space Physics Laboratory (SPL), VSSC, Trivandrum, India.

⁴Masdar Institute of Science and Technology, Abu Dhabi, UAE.

⁵CEBROSS, Chennai, India.

*vratnam@narl.gov.in , 08585-272123 (phone), 08585-272018 (Fax)



23 **Abstract**

24 Tropical cyclones play an important role in modifying the tropopause structure and
25 dynamics as well as stratosphere-troposphere exchange (STE) process in the Upper
26 Troposphere and Lower Stratosphere (UTLS) region. In the present study, the impact of
27 cyclones that occurred over the North Indian Ocean during 2007-2013 on the STE process is
28 quantified using satellite observations. Tropopause characteristics during cyclones are
29 obtained from the Global Positioning System (GPS) Radio Occultation (RO) measurements
30 and ozone and water vapor concentrations in UTLS region are obtained from Aura-
31 Microwave Limb Sounder (MLS) satellite observations. The effect of cyclones on the
32 tropopause parameters is observed to be more prominent within 500 km from the centre of
33 cyclone. In our earlier study we have observed decrease (increase) in the tropopause altitude
34 (temperature) up to 0.6 km (3K) and the convective outflow level increased up to 2 km. This
35 change leads to a total increase in the tropical tropopause layer (TTL) thickness of 3 km
36 within the 500 km from the centre of cyclone. Interestingly, an enhancement in the ozone
37 mixing ratio in the upper troposphere is clearly noticed within 500 km from cyclone centre
38 whereas the enhancement in the water vapor in the lower stratosphere is more significant on
39 south-east side extending from 500 -1000 km away from the cyclone centre. We estimated
40 the cross-tropopause mass flux for different intensities of cyclones and found that the mean
41 flux from stratosphere to troposphere for cyclonic storms is $0.05 \pm 0.29 \times 10^{-3} \text{kgm}^{-2}$ and for very
42 severe cyclonic storms it is $0.5 \pm 1.07 \times 10^{-3} \text{kgm}^{-2}$. More downward flux is noticed in the north-
43 west and south-west side of the cyclone centre. These results indicate that the cyclones have
44 significant impact in effecting the tropopause structure, ozone and water vapour budget and
45 consequentially the STE in the UTLS region.

46

47 **Keywords:** Tropical cyclone, tropopause, ozone, water vapor, STE processes.



48 **1. Introduction**

49 Tropical cyclones with deep convective synoptic scale systems persisting for a few
50 days to weeks play an important role on the mass exchange between troposphere and
51 stratosphere and vice versa. They transport large amount of water vapor, energy and
52 momentum to the upper troposphere and lower stratosphere (UTLS) region. Cyclones provide
53 favorable conditions for entry of the water vapour-rich and ozone-poor air from surface to the
54 lower stratosphere (LS) and water vapor- poor and ozone-rich air from the LS to the upper
55 troposphere (UT) leading to the stratosphere-troposphere exchange (STE) (Zhan and Wang,
56 2012; Romps and Kuang, 2009; Vogel et al., 2014). These exchanges occur mainly around
57 the tropopause and change the thermal and chemical structure of the UTLS region. The
58 concentration of the water vapour transported from troposphere to stratosphere is controlled
59 by the cold temperatures present at the tropopause and this is a major factor in the STE
60 (Fueglistaler et al., 2009). The transport of water vapour and ozone around the tropopause
61 caused by the cyclones can affect the radiation balance of the atmosphere.

62 Increase of water vapor in the LS region will leads to a warming and ozone loss in
63 this atmospheric region (Stenke and Grewe, 2005). In general, most of the air enters into the
64 stratosphere over the tropics (Brewer, 1949; Dobson, 1956). As suggested by Newell and
65 Gould-Stewart (1981), Bay-of-Bengal is one of the active regions where troposphere air
66 enters into the stratosphere. It is also one of the active regions for the formation of deep
67 convection associated cyclones which contains strong updrafts. Earlier studies have shown a
68 close relationship between cyclones and moistening of the upper troposphere (Wang et al.,
69 1995; Su et al., 2006; Ray and Rosenlof, 2007).

70 Several studies have been carried out related to water vapor, ozone transport as well
71 as STE processes around the UTLS region during cyclones. Koteswaram (1967) described
72 the thermal and wind structure of cyclones in the UTLS region with the major findings of



73 cold core persisting just above the 15 km and the outflow jets very close to the tropopause.
74 Penn (1965) reported enchantment in ozone and warmer air situated above the tropopause
75 over the eye region during hurricane Ginny. Waco (1970) observed turbulent conditions at
76 the cloud top level and large vertical temperature gradient occurring above the tropopause
77 during hurricane Beulaw. Danielsen (1993) reported on troposphere-stratosphere transport
78 and dehydration in the lower tropical stratosphere during cyclone period. Baray et al. (1999)
79 studied the STE during cyclone Marlene and they observed maximum of ozone change at 300
80 hPa level. Zou and Wu (2005) observed the variations of columnar ozone in different stages
81 of hurricane by using satellite measurements. Bellevue et al. (2007) observed increase in O₃
82 concentration in the upper troposphere during TC event. Significant contribution of cyclones
83 on hydration of the UT is reported by Ray and Rosenlof (2007) and injection of tropospheric
84 air into the low stratosphere due to overshooting convection by cyclones is reported by
85 Romps and Kuang (2009). Das (2009) studied the stratospheric intrusion into troposphere
86 during the passage of cyclone by using MST Radar observations. Strong enhancement of O₃
87 in the upper troposphere is observed during TCs over BoB (Fadnavis et al., 2011). The
88 increased O₃ levels in the boundary layer as well as near surface by as much as 20 to 30 ppbv
89 due to strong downward transport of O₃ in the tropical convection is also observed (Betts et
90 al., 2002; Sahu and Lal, 2006; Grant et al., 2008). More literature related to influence of
91 cyclones on the UTLS structure and composition is presented in Cairo et al. (2008). Biondi et
92 al. (2013) presented the method to estimate the cloud top height and vertical temperature
93 structure during cyclones using Global Position System (GPS) Radio Occultation (RO)
94 measurements. Biondi et al. (2015) also studied the thermal structure of cyclones over
95 different Ocean basins using the same measurements. Ravindra Babu et al. (2015) reported
96 the effect of cyclones on the tropical tropopause parameters using COSMIC GPS RO data.
97 Many studies have been carried out on the role of extra tropical cyclones on the STE (for



98 example Reutter et al., 2015 and references therein) though the quantitative estimates of STE
99 provided by these case studies varied considerably. However, the vertical and horizontal
100 variation of ozone and water vapor in the UTLS region and cross-tropopause flux
101 quantification during cyclones over north Indian Ocean is not well investigated.

102 In the present study, we investigate the spatial and vertical variations of ozone and
103 water vapor in the UTLS region for all the cyclones occurred over north Indian Ocean during
104 2007 to 2013 by using Aura- Microwave Limb Sounder (MLS) satellite observations. The
105 effect of cyclones on the tropopause characteristics is also presented using COSMIC GPS RO
106 measurements. We also present the cross-tropopause mass flux estimated for each of the
107 cyclones.

108 2. Data and Methodology

109 In the present study, we used Aura –MLS water vapor and ozone measurements
110 (version 3.3) provided by the Jet Propulsion Laboratory (JPL). The version 3.3 was released
111 in January 2011 and this updated version has change in the vertical resolution. The vertical
112 resolution of the water vapor is in the range 2.0 to 3.7 km from 316 to 0.22 hPa and along
113 track horizontal resolution varies from 210 to 360 km for pressure greater than 4.6 hPa. For
114 ozone, vertical resolution is ~2.5 km and the along track horizontal resolution varies between
115 300 and 450 km (Livesey et al., 2011). The Aura MLS gives around 3500 vertical profiles per
116 day and it crosses the equator at 1:40 am and 1:40 pm local time. For calculating the cross-
117 tropopause mass flux, we used ERA-Interim winds obtained during cyclone period. We
118 adopted method given by Wie (1987) to estimate the cross tropopause mass flux, F . F is
119 defined as:

$$120 \quad F = \frac{1}{g} \left(-\omega + V_h \cdot \nabla P_{tp} + \frac{\partial P_{tp}}{\partial t} \right) = \left(-\frac{\omega}{g} + \frac{1}{g} V_h \cdot \nabla P_{tp} \right) + \frac{1}{g} \frac{\partial P_{tp}}{\partial t} = F_{AM} + F_{TM} \quad (1)$$



121 Where ω is the vertical pressure-velocity, V_h is the horizontal vector wind, P_{tp} is the pressure at
122 the tropopause, g is the acceleration due to gravity, F_{AM} is the air mass exchange due to
123 horizontal and vertical air motions, F_{TM} is the air mass exchange due to tropopause motion.

124 We have taken the cyclone track information data from India Meteorological Department
125 (IMD) best track data from year 2007-2013. During this period, around 50 cyclones have
126 formed over north Indian Ocean. Due to the considerable variability of cyclone life-cycles,
127 for the present study we selected only 16 cyclones that lasted for more than 4 days. TCs over
128 north Indian ocean are classified in different categories by IMD based on their maximum
129 sustained wind speed as low pressure when the maximum sustained wind speed at the sea
130 surface is < 17 knots/32 kmph, as depression (D) at 17–27 knots/32–50 kmph, deep
131 depression (DD) at 28–33 knots/51–59 kmph, cyclonic storm (CS) at 34– 47 knots/60–90
132 kmph, severe cyclonic storm (SCS) at 48–63 knots/90–110 kmph, very severe cyclonic storm
133 (VSCS) at 64–119 knots/119–220 kmph, and super cyclonic storm (SuCS) at > 119 knots/220
134 kmph respectively (Pattnaik and RamaRao, 2008). The mean sustained time for cyclones that
135 occurred during pre-monsoon season is 101.14 ± 49.7 hours and for post-monsoon season is
136 112.6 ± 29.47 hours. Out of 16 cyclones, 7 cyclones (CS(2), SCS(2), VSCS(2) and SuCS(1))
137 formed during pre-monsoon season and 9 cyclones (CS(1), SCS(2), and VSCS(6)) formed
138 during post-monsoon season. Depressions and deep depressions are not considered. Since
139 there are (temporal) limitations in the satellite measurements we considered mean cross
140 tropopause flux for the cyclones that lasted for more than 4 days. However, our quantification
141 of cross tropopause flux will not be affected by this limitation as earlier studies revealed that
142 maximum STE occurs during mature to peak stage of cyclone. Details on the selection of 16
143 cyclones are presented in Ravindra Babu et al. (2015). The tracks of all the cyclones used for
144 the present study are shown in Figure 1 and different colors indicate different categories of
145 the cyclones.



146 As shown in equation 1, for estimating the cross tropopause flux we need information on the
147 tropopause parameters. We used post-processed products of level 2 dry temperature profiles
148 with vertical resolution around 200 m provided by the COSMIC Data Analysis and Archival
149 Center (CDAAC) for estimating the tropopause parameters during cyclones period from
150 2007-2013. COSMIC GPS RO is a constellation of six microsattelites equipped with GPS
151 receivers (Anthes et al., 2008). We also used CHALLENGING Minisatellite Payload (CHAMP)
152 GPS RO data that are available between the years 2002 to 2006 and COSMIC Data from
153 2007-2013 for getting background climatology of tropopause parameters over north Indian
154 Ocean.

155 **3. Results and discussion**

156 **3.1. Tropopause characteristics observed during cyclones**

157 As mentioned earlier, in the tropical region the amount of water vapor transported in
158 to the stratosphere from the troposphere is controlled by the cold temperatures present at the
159 tropopause (Fueglistaler et al., 2009). Large convection around the eye and strong updrafts
160 near the eye-walls transports large amount of water vapor in to the stratosphere through the
161 tropopause. In this way, cyclones will affect the tropopause structure (altitude/temperature).
162 Climatological mean of all the tropopause parameters are obtained by combining GPS RO
163 measurements obtained from CHAMP and COSMIC (2002-2013). The tropopause
164 parameters include cold point tropopause altitude (CPH) and temperature (CPT), lapse rate
165 tropopause altitude (LRH) and temperature (LRT) and the thickness of the tropical
166 tropopause layer (TTL), defined as the layer between convective outflow level (COH) and
167 CPH and are calculated for each profile of GPS RO collected during the above mentioned
168 period. All the tropopause parameters mentioned above are calculated for each occultation
169 that is available during cyclone period within 1000 km from the centre. These individual
170 tropopause parameters are subtracted from the climatological mean of tropopause parameters



171 to estimate the effect of TCs on the tropopause. We also calculated the difference of
172 tropopause parameters for different cyclone intensities (Figures are not shown). Figure 2
173 shows the cyclone centered – composite of mean difference in the tropopause parameters
174 (CPH, LRH, CPT, LRT, COH and TTL thickness) between climatological mean (2002-2013)
175 and individual tropopause parameters observed during cyclones(irrespective of cyclone
176 intensity) and the detailed methodology for plotting Fig.2 can be found in Ravindra Babu et
177 al. (2015). We have reported that the CPH (LRH) is lowered by 0.6 km (0.4 km) in most of
178 the areas within the 500 km radius from the cyclone centre and the temperature (CPT/LRT) is
179 more or less colder or equal to the climatological values from the area around 1000 km from
180 the cyclone centre. Note that effect of cyclone can be felt up to 2000 km but since latitudinal
181 variation also comes into picture when we consider 2000 km radius, we restrict our
182 discussion related to variability within 1000 km from the cyclone centre. COH (TTL
183 thickness) has increased (reduced) up to 2 km within 500 km from the cyclones in some areas
184 up to 1000 km. Note that this decrease in TTL thickness is not only because of pushing up of
185 the COH but also due to decrease of CPH. From the above results, we concluded that the
186 tropical tropopause is significantly affected by the cyclones and the effect is more prominent
187 within 500 km from the cyclone centre. These changes in tropopause parameters are expected
188 to influence the water vapor and ozone transport in the UTLS during cyclones.

189 **3.2. Ozone variability in the UTLS region during cyclones**

190 To see the variability and the transport of ozone during cyclones, we investigated the
191 spatial and vertical variability of ozone in the UTLS region using MLS satellite observations.
192 We separated the MLS overpasses based on the distance from the TC centre and Figure 3
193 shows the normalized cyclone centered – composite of mean ozone mixing ratio (OMR)
194 observed during cyclones(irrespective of cyclone intensity) at 82hPa, 100hPa, 121hPa, and
195 146 hPa pressure levels during 2007-2013. Black circles are drawn to show distances 250 km,



196 500 km, 750 km and 1000 km away from cyclone center. Since large variability in OMR is
197 noticed from one pressure level to other, we normalized the values to the highest OMR value
198 at a given pressure level. The highest OMR values at 82 hPa, 100 hPa, 121 hPa and 146 hPa
199 pressure levels is 0.38 ppmv, 0.28 ppmv, 0.19 ppmv and 0.13 ppmv, respectively. Large
200 spatial variations in the OMR are observed with respect to the cyclone centre. At 82 hPa,
201 higher OMR (~0.4 ppmv) in the South-West (SW) side up to 1000 km and comparatively low
202 OMR values (~0.2 ppmv) are noticed in the north of the cyclone centre. At 100 hPa, an
203 increase in the OMR (~0.2 ppmv) near the cyclone centre within 500 km is clearly observed.
204 This enhancement in OMR extends up to 146 hPa and is more prominent slightly in the
205 western and eastern side of cyclone. In general, the large subsidence located at the top of the
206 cyclone centre is expected to bring lower stratospheric ozone to the upper troposphere. This
207 is the reason for the enhancement of ozone in the cyclone centre within 500 km. Interestingly,
208 an enhancement in OMR in south east side at 121 hPa but is not either at 100 hPa or at 146
209 hPa can be noticed which need to be investigated further. Thus in general, higher ozone
210 concentrations are observed in cyclone centre within 500 km and slightly aligned to the
211 western side of the cyclone centre.

212 In order to quantify the impact of cyclones on UTLS ozone more clearly we have
213 obtained anomalies by subtracting the mean cyclone-centered ozone observed during
214 cyclones from the background climatology of UTLS ozone. Figure 3 (e-h) shows the
215 normalized mean difference of cyclone-centered ozone obtained after removing the
216 background climatology values for different pressure levels shown in Figure 3 (a-d). The
217 maximum difference in OMR for corresponding normalized value at 82 hPa, 100 hPa, 121
218 hPa and 146 hPa pressure levels is -0.089 ppmv, -0.19 ppmv, -0.09 ppmv and -0.06 ppmv,
219 respectively. Enhancement in the OMR (~0.1 ppmv) up to 1000 km from the cyclone centre
220 is observed at 82 hPa. Interestingly, at 100 hPa OMR is more or less uniform throughout



221 1000 km from the cyclone centre except ~500 km radius from the centre where significant
222 increase of OMR (~0.2 ppmv) is observed. This increase in the OMR is within 500 km from
223 cyclone centre and extends up to 121 hPa. However, enhancement in OMR at 146 hPa
224 extends up to 1000 km but distributed towards eastern and western sides of cyclone centre.
225 Thus, it is clear that the detrainment of lower stratospheric ozone will reach up to 146 hPa
226 during cyclone period due to presence of strong subsidence in the cyclone centre. We do not
227 know what happens below this pressure level due to limitation in the present data, however,
228 studies (Das et al., 2015; Jiang et al., 2015) have shown that LS ozone can reach low as
229 boundary layer during cyclones. It will be interesting to see the variability in the water vapor
230 as large amount of it is expected to cross the tropopause during the cyclone period and reach
231 lower stratosphere.

232 3.3. Water vapor variability in the UTLS region during cyclones

233 As mentioned earlier, enormous amount of water vapor is expected to be pumped
234 from lower troposphere to the upper troposphere and even up to the lower stratosphere during
235 cyclones. To see the linkage between tropopause variability and the transport of water vapor
236 during cyclones, we investigated the horizontal and vertical variability of water vapor in the
237 UTLS region using same MLS satellite observations. Figure 4 shows the normalized cyclone
238 centered – composite of mean water vapor mixing ratio observed during cyclones
239 (irrespective of cyclone intensity) at 82hPa, 100hPa, 121hPa, and 146 hPa pressure levels
240 observed by MLS during 2007-2013. Black circles are drawn to shown the 250 km, 500 km,
241 750 km and 1000 km away from cyclone center. The highest Water Vapor Mixing Ratio
242 (WVMR) values for corresponding normalized value at 82 hPa, 100 hPa, 121 hPa, and 146
243 hPa pressure levels is 4.44 ppmv, 4.49 ppmv, 6.9 ppmv and 16.03 ppmv, respectively.
244 Significantly higher WVMR values are noticed extending from 500 km up to 1000 km from
245 the cyclone centre at 121 (~6.5 ppmv), 146 hPa (~15 ppmv) levels with more prominence in



246 the eastern side of the cyclone centre. Comparatively low values are noticed in the centre of
247 the cyclone especially at 121 hPa. These results match well with higher WVMR observed in
248 the eastern side of cyclones over Atlantic and Pacific Oceans (Ray and Rosenlof, 2007).
249 These results also match with those reported by Ravindra Babu et al. (2015) where they used
250 GPS RO measured relative humidity and found enhancement in RH in the eastern side of the
251 centre in the upper troposphere (10-15 km) over north Indian Ocean. The higher WVMR
252 values are observed in the eastern side of the cyclone centre might be due to the upper level
253 anti-cyclonic circulation over the cyclones. It is interesting to note that high WVMR lies not
254 at the centre but extend from 500 to 1000 km from the centre of cyclone. The WVMR show
255 high at 121 and 146 hPa than at 100 and 82 hPa. It seems less water vapor has been
256 transported to 100 and 82 hPa from below. As we know, water vapor mostly origin from
257 lower troposphere and decreasing with height. So vertical transport of water vapor from
258 lower troposphere to UTLS may lead to water vapor enhanced at 121 and 146 hPa and some
259 it reaches at higher altitudes. The higher WV MR presented at 100 and 82 hPa levels show
260 the signature of the tropospheric air entering even in to the lower stratosphere during
261 cyclones.

262 In order to quantify the impact of cyclones on UTLS water vapor more clearly we
263 have obtained anomalies by subtracting the mean cyclone-centered water vapor observed
264 during cyclones from the background climatology of UTLS water vapor. Figure 4 (e-h)
265 shows the normalized mean difference of cyclone-centered WVMR obtained after removing
266 the background climatology values for different pressure levels shown in Figure 4 (a-d). The
267 maximum difference in WVMR for corresponding normalized values at 82 hPa, 100 hPa, 121
268 hPa, and 146 hPa pressure levels is -0.44 ppmv, -0.81 ppmv, -2.55 ppmv and -9.09 ppmv,
269 respectively. More than 7 ppmv differences are observed at 146 hPa within the 1000 km from
270 the centre and at 121 hPa difference of ~ 2 ppmv is noticed extending up to 2000 km (figure



271 not shown) in the eastern side of the centre. At 100 hPa and 82 hPa levels, the increase in the
272 WVMR is ~ 0.8 and ~ 0.6 ppmv, respectively, and the enhancement is more observed in the
273 NE side of the centre. Thus, a clear stratosphere- troposphere exchange (STE) is evident
274 during the cyclone over north Indian Ocean where a clear enhancement in the water vapor
275 (ozone) in the lower stratosphere (upper troposphere) is observed. For quantifying the amount
276 of STE, we calculated the cross-tropopause mass flux for each cyclone by considering the
277 spatial extent within the 500 km from the cyclone centre and results are presented in the
278 following sub-section.

279 **3.4. Cross tropopause flux observed during cyclones**

280 As mentioned in Section 2, the method proposed by Wie (1987) is used to estimate
281 the cross-tropopause mass flux (equation 1) during cyclones. Since the above mentioned
282 results showed that the higher OMR values are observed in the west and NW side and more
283 water vapor is located at the eastern side of the cyclone centre, we separated the area into 4
284 sectors with respect to cyclone centre as C1 (NW side), C2 (NE side), C3 (SW side), and C4
285 (SE side), respectively which are shown in Figure 3(a). Table 1 presents the different cyclones
286 used in the present study with their names, cyclone intensity (CI), centre latitude, centre
287 longitude, minimum estimated central pressure on their peak intensify day. The total flux F
288 (equation 1) depends on the air mass exchange due to horizontal and vertical air motion
289 (F_{AM}), and the air mass exchange due to tropopause motion itself (F_{TM}). Since number of GPS
290 RO measurements are not sufficient to estimate the second term (F_{TM}) for each event, we
291 calculated only the first part of the equation (F_{AM}) individually for each of cyclone with
292 respect to different sectors mentioned above and the values are presented in Table
293 1. However, we roughly estimated the contribution of second term by assuming change in the
294 tropopause pressure by 0.5 hPa increase (decrease) within 6 h and could see cross-tropopause
295 flux for CS is $0.25 \pm 0.07 \times 10^{-3} \text{kgm}^{-2}\text{s}^{-1}$ ($-0.36 \pm 0.07 \times 10^{-3} \text{kgm}^{-2}\text{s}^{-1}$) and for VSCS it is -



296 $0.24 \pm 0.3 \times 10^{-3} \text{kgm}^{-2} \text{s}^{-1} (-0.85 \pm 0.3 \times 10^{-3} \text{kgm}^{-2} \text{s}^{-1})$. If there is change in the tropopause pressure
297 by 1 hPa increase (decrease), the flux for CS is $0.55 \pm 0.07 \times 10^{-3} \text{kgm}^{-2} \text{s}^{-1} (-0.66 \pm 0.07 \times 10^{-3} \text{kgm}^{-2}$
298 $\text{s}^{-1})$ and for VSCS it is $0.06 \pm 0.3 \times 10^{-3} \text{kgm}^{-2} \text{s}^{-1} (-1.16 \pm 0.3 \times 10^{-3} \text{kgm}^{-2} \text{s}^{-1})$.

299 Figure 5 shows the cross-tropopause flux estimated in the C1 (NW), C2 (NE), C3
300 (SW), and C4 (SE) sectors from the centre of cyclone for different cyclone intensities
301 (estimated based on cyclone centre pressure). Red lines show the best fit. It clearly shows that
302 the downward flux is always more in C1 and C3 sectors where as C2 sector show more
303 upward flux. The flux itself varies with the cyclone intensity and we could see an increase in
304 the downward flux as the cyclone centre pressure decreases particularly during C1 and C3
305 sectors. Whereas in the C4 sector, increase in the upward flux is seen as the cyclone intensity
306 increases but always upward in the C2 sector, irrespective of the cyclone intensity. The
307 second term (in equation 1) itself corresponds the air mass exchange from the tropopause
308 motion and generally during cyclone period there is an ~ 400 m difference in tropopause
309 altitude (LRH) within 500 km from the centre of the cyclone (Ravindra Babu et al., 2015).
310 Thus, spatial and temporal variation of tropopause during cyclones itself is very important for
311 to decide the flux as downward or upward. Interestingly C1 (NW) and C3 (SW) sectors of
312 cyclone show dominant downward mean flux and C2 (NE) and C4 (SE) sectors show
313 dominant upward mean flux with the values of $0.4 \pm 0.4 \times 10^{-3} \text{kgm}^{-2}$, $1.2 \pm 1.0 \times 10^{-3} \text{kgm}^{-2}$,
314 $0.2 \pm 0.1 \times 10^{-3} \text{kgm}^{-2}$ and $0.12 \pm 0.3 \times 10^{-3} \text{kgm}^{-2}$, respectively. These results strongly support our
315 findings of higher ozone in the NW and SW sides and higher water vapor in the NE side of
316 the cyclone centre. The mean flux is observed to vary with the intensity of the cyclone. Mean
317 flux for severe cyclonic storms (CS) is $-0.05 \pm 0.29 \times 10^{-3} \text{kgm}^{-2}$ whereas for very severe
318 cyclonic storms (VSCS) it is $-0.5 \pm 1.07 \times 10^{-3} \text{kgm}^{-2}$. Reutter et al. (2015) reported the upward
319 and downward mass fluxes across the tropopause are more dominant in deeper cyclones
320 compared to less intense cyclones for North Atlantic cyclones. Our results match fairly well



321 with their results with the averaged mass flux of stratosphere to troposphere as $0.3 \times 10^{-3} \text{ kg m}^{-2}$
322 s^{-1} ($340 \text{ kg km}^{-2} \text{ s}^{-1}$) in the vicinity of cyclones over the North Atlantic Ocean.

323 4. Summary and conclusions

324 In this study we have investigated the vertical and spatial variability of ozone and
325 water vapor in the UTLS region during cyclones occurred between 2007 and 2013 over the
326 North Indian Ocean by using Aura-MLS satellite observations. In order to make quantitative
327 estimate of the impact of cyclones on the ozone and water vapor budget in the UTLS region,
328 we removed the mean cyclone-centre ozone and water vapor from the climatological mean
329 calculated using MLS data from 2007 to 2013. We estimated the mean cross-tropopause flux
330 for each of the cyclones on their peak intensify day. We also presented the spatial variability
331 of the tropopause parameters during cyclones by using the high vertical resolution and high
332 accuracy COSMIC GPS RO measurements. We used background climatology of tropopause
333 parameters calculated by using GPS RO measurements available from 2002 and 2013
334 (CHAMP+COSMIC) for estimating the effect of cyclones on tropopause parameters. The
335 main findings of the present communication are summarized below.

- 336 1. Lowering of CPH (0.6 km) and LRH (0.4 km) values with coldest CPT and LRT (2–3
337 K) within a 500 km radius from the cyclone centre is noticed. Higher (2 km) COH
338 leading to the lowering of TTL thickness (~3 km) is clearly observed (Ravindra Babu
339 et al., 2015).
- 340 2. The impact of cyclones on the ozone and the tropopause (altitude/temperature) is
341 more prominent within 500 km from the cyclone centre whereas it is high from 500
342 km to 1000km in case of water vapor.
- 343 3. Detrainment of ozone is highest in the cyclone centre (within 500 km from the centre)
344 due to strong subsidence over top of the cyclone centre and this detrained ozone
345 reaches as low as 146 hPa level (~13-14 km).



346 4. Interestingly significant enhancement in the lower stratosphere (82 hPa) water vapor
347 is noticed in the east and SE side from the cyclone centre.

348 5. Dominant downward [upward] cross-tropopause flux is observed in the C1 (NW) and
349 C3 (SW)[C2 (NE) and C4 (SE)] sectors of cyclone.

350 Figure 6 depicts above mentioned results in the form of the schematic diagram. The
351 tropopause altitude (CPH) is lowered by 0.6 km within 500 km from the centre of cyclone.
352 The convective out flow level (COH) slightly pushes up (~2 km) with in 500 km from the
353 centre of cyclone but not exactly in the centre. Thus, a decrease of about 3 km in the TTL
354 thickness is observed within the 500 km from the cyclone centre. Cyclone includes eye that
355 extends from few km to 10's of kilometers. Strong convective towers with strong updrafts
356 extending up to the tropopause altitude in the form of spiral bands extending from 500 to
357 1000 km are present. Strong water vapor transport in to the lower stratosphere (82 hPa) while
358 pushing up the COH is observed around these spiral bands in the present study. Between
359 these spiral bands equal amount of subsidence is expected with strong subsidence existing at
360 the centre of the cyclone. Significant detrainment of ozone present above or advected from
361 the surroundings is observed reaching as low as 146 hPa at the cyclones centre. Thus, it is
362 clear that ozone reaches upper troposphere from lower stratosphere through the centre of the
363 cyclone whereas water vapor transport in to the lower stratosphere will happen from the 500
364 to 1000 km from the cyclones centre. Since more intensity cyclones are expected to occur in
365 a changing climate (Kuntson et al., 2010), the amount of water vapor and ozone reaching
366 lower stratosphere and upper troposphere, respectively, is expected to increase thus effecting
367 complete tropospheric weather and climate. Future studies should focus on these trends.

368

369 **Acknowledgements:** We would like to thank COSMIC Data Analysis and Archive Centre
370 (CDAAC) for providing GPS RO data used in the present study through their FTP site



371 (<http://cdaac-www.cosmic.ucar.edu/cdaac/products.html>). The provision of tropical cyclone
372 best track data used in the present study by IMD through their website
373 (<http://www.imd.gov.in/section/nhac/dynamic/cyclone.htm>) and Aura-MLS observations
374 obtained from the GES DISC through their ftp site (<https://mls.jpl.nasa.gov/index-eos-mls.php>)
375 is highly acknowledged. This work is supported by Indian Space Research
376 Organization (ISRO) through CAWSES India Phase-II Theme 3 programme.



377 **References:**

- 378 Anthes, R. A., Bernhardt, P. A., Chen, Y., Cucurull, L., Dymond, K. F., Ector, D., Healy, S.
379 B., Ho, S.-H., Hunt, D. C., Kuo, Y.-H., Liu, H., Manning, K., McCormick, C., Meehan, T.
380 K., Randel, W. J., Rocken, C., Schreiner, W. S., Sokolovskiy, S. V., Syndergaard, S.,
381 Thompson, D. C., Trenberth, K. E., Wee, T.-K., Yen, N. L., and Zeng, Z.: The
382 COSMIC/Formosat/3 mission: Early results, *B. Am. Meteorol. Soc.*, 89, 313–333, 2008.
- 383 Baray, J. L., Ancellet, G., Radriambelo T., and Baldy, S.: Tropical cyclone Marlene and
384 stratosphere-troposphere exchange, *J. Geophys. Res.*, 104, 13,953–13,970,
385 doi:10.1029/1999JD900028-1999.
- 386 Bellevue, J., Baray, J. L., Baldy, S., Ancellet, G., Diab, R. D., and Ravetta, F.: Simulations of
387 stratospheric to tropospheric transport during the tropical cyclone Marlene event, *Atmos.*
388 *Environ.*, 41, 6510–6526, doi:10.1016/j.atmosenv.2007.04.040, 2007.
- 389 Betts, A. K., Gatti, L. V., Cordova, A. M., Silva Dias, M. A. F., and Fuentes, J. D.: Transport
390 of ozone to the surface by convective downdrafts at night, *J. Geophys. Res.*, 107, 8046,
391 doi:10.1029/2000JD000158, 2002.
- 392 Biondi, R., Ho, S. P., Randel, W., Syndergaard, S., and Neubert, T.: Tropical cyclone cloud-
393 top height and vertical temperature structure detection using GPS radio occultation
394 measurements, *J. Geophys. Res. Atmos.*, 118, 5247–5259, doi:10.1002/jgrd.50448, 2013.
- 395 Biondi, R., Steiner, A. K., Kirchengast, G., and Rieckh, T.: Characterization of thermal
396 structure and conditions for overshooting of tropical and extratropical cyclones with GPS
397 radio occultation, *Atmos. Chem. Phys.*, 15, 5181–5193, doi:10.5194/acp-15-5181- 2015,
398 2015.



- 399 Brewer, A. W.: Evidence for a world circulation provided by the measurements of helium
400 and water vapor distribution in the stratosphere. *Quarterly Journal of Royal Meteorological*
401 *Society.*, 75, 351–363, doi:10.1002/qj.49707532603-1949.
- 402 Cairo, F., Buontempo, C., MacKenzie, A. R., Schiller, C., Volk, C. M., Adriani, A., Mitev,
403 V., Matthey, R., Di Donfrancesco, G., Oulanovsky, A., Ravegnani, F., Yushkov, V., Snels,
404 M., Cagnazzo, C., and Stefanutti, L.: Morphology of the tropopause layer and lower
405 stratosphere above a tropical cyclone: a case study on cyclone Davina (1999), *Atmos.*
406 *Chem. Phys.*, 8, 3411– 3426, doi:10.5194/acp-8-3411-2008, 2008.
- 407 Danielsen, E. F.: In situ evidence of rapid, vertical, irreversible transport of lower
408 tropospheric air into the lower tropical stratosphere by convective cloud turrets and by
409 larger-scale upwelling in tropical cyclones, *J. Geophys. Res.*, 98, 8665–8681, doi:
410 10.1029/92JD02954-1993.
- 411 Das, S. S.: A new perspective on MST radar observations of stratospheric intrusions into
412 troposphere associated with tropical cyclone. *Geophys. Res. Lett.*, 36, L15821, doi:
413 10.1029/2009GL039184-2009.
- 414 Das, S.S., Ratnam, M. V., Uma, K.N., Subrahmanyam, K.V., Girach, I.A., Patra, A.K.,
415 Aneesh, S., Suneeth, K.V., Kumar, K.K., Kesarkar, A.P., Sijikumar, S., and Ramkumar,
416 G.: Influence of Tropical Cyclone on Tropospheric Ozone: Possible Implication, *Atmos.*
417 *Chem. Phys. Discuss.*, 15, 19305-19323, 2015.
- 418 Dobson, G. M. B.: Origin and Distribution of the Polyatomic Molecules in the Atmosphere,
419 *Royal Society of London Proceedings Series A*, 236, 187–193,
420 doi:10.1098/rspa.1956.0127, 1956.
- 421 Fadnavis, S., Berg, G., Buchunde, P., Ghude, S. D., and Krishnamurti, T. N.: Vertical
422 transport of ozone and CO during super cyclones in the Bay of Bengal as detected by



- 423 Tropospheric Emission Spectrometer, *Environ. Sci. Pollut. R.*, 18, 301–315,
424 doi:10.1007/s11356-010-0374-3, 2011.
- 425 Fueglistaler, S., Dessler, A. E., Dunkerton, T. J., Fu, I., Folkins, Q., and Mote, P. W.:
426 Tropical tropopause layer, *Rev. Geophys.*, 47, RG1004, doi:10.1029/2008RG000267, 2009.
- 427 Grant, D. D., Fuentes, J. D., DeLonge, M. S., Chan, S., Joseph, E., Kucera, P., Ndiaye, S. A.,
428 and Gaye, A. T.: Ozone transport by mesoscale convective storms in western Senegal,
429 *Atmos. Environ.*, 42, 7104–7114, doi:10.1016/j.atmosenv.2008.05.044, 2008.
- 430 Jiang, Y.C., Zhao, T.L., Liu, J., Xu, X.D., Tan, C.H., Cheng, X.H., Bi, X.Y., Gan, J.B., You,
431 J.F., and Zhao, S.Z.: Why does surface ozone peak before a typhoon landing in
432 southeast China? *Atmos. Chem. Phys.*, 15, 13331–13338, 2015
- 433 Koteswaram, P.: On the structure of hurricanes in the upper troposphere and lower
434 stratosphere, *Mon. Weather Rev.*, 95, 541–564, 1967.
- 435 Knutson, T.R., John, L., McBride, Johnny Chan, Kerry Emanuel, Greg Holland, Chris
436 Landsea, Isaac Held, James P. Kossin, Srivastava, A.K., and Masato Sugi: Tropical
437 cyclones and climate change, *Nature Geosci.*, 3, 157 – 163, 2010.
- 438 Livesey, N., Read, W. G., Frovideaux, L., Lambert, A., Manney, G. L., Pumphrey, H. C.,
439 Santee, M. L., Schwartz, M. J., Wang, S., Cofield, R. E., Cuddy, D. T., Fuller, R. A.,
440 Jarnot, R. F., Jiang, J. H., Knosp, B. W., Stek, P. C., Wagner, P. A., and Wu, D. L.: Earth
441 Observing System (EOS) Aura Microwave Limb Sounder (MLS) Version 3.3 Level 2 data
442 quality and description document, JPL D-33509, JPL publication, USA, 2011.
- 443 Newell, R. E., and Gould-Stewart, S.: A stratospheric fountain, *Journal of Atmospheric*
444 *Science.*, 38, 2789–2796, doi:10.1175/1520-0469-1981.
- 445 Pattnaik, D. R. and Rama Rao, Y. V.: Track Prediction of very severe cyclone “Nargis” using
446 high resolution weather research forecasting (WRF) model, *J. Earth Syst. Sci.*, 118, 309–
447 329, 2008.



- 448 Penn, S.: Ozone and temperature structure in a Hurricane, *J. Appl. Meteorol.*, 4, 212–216,
449 1965.
- 450 RavindraBabu,S., VenkatRatnam, M., Basha, G., Krishnamurthy. B.V. and Venkateswara
451 Rao, B.: Effect of tropical cyclones on the tropical tropopause parameters observed using
452 COSMIC GPS RO data. *Atmos. Chem. Phys.*, 15, 10239-10249, doi: 10.5194/acp-15-
453 10239-2015.
- 454 Ray, E. A. and Rosenlof, K. H.: Hydration of the upper troposphere by tropical cyclones, *J.*
455 *Geophys. Res.*, 112, D12311, doi:10.1029/2006JD008009, 2007.
- 456 Reutter, P., Škerlak, B., Sprenger, M., and Wernli, H.: Stratosphere-troposphere exchange
457 (STE) in the vicinity of North Atlantic cyclones. *Atmos. Chem. Phys.*, 15, 10939–10953,
458 2015.
- 459 Romps, D. M. and Kuang, Z. M.: Overshooting convection in tropical cyclones, *Geophys.*
460 *Res. Lett.*, 36, L09804, doi:10.1029/2009GL037396, 2009.
- 461 Sahu, L. K. and Lal, S.: Changes in surface ozone levels due to convective downdrafts over
462 the Bay of Bengal, *Geophys. Res. Lett.*, 33, L10807, doi:10.1029/2006GL025994, 2006.
- 463 Stenke, A. and Grewe, V.: Simulation of stratospheric water vapor trends: impact on
464 stratospheric ozone chemistry. *Atmos. Chem. Phys.*, 5, 1257–1272, doi: 10.5194/acp-5-
465 1257-2005.
- 466 Su, H., Read, W.G., Jiang, J. H., Waters, J. W., Wu, D. L., and Fetzer, E. J.: Enhanced
467 positive water vapor feedback associated with tropical deep convection: New evidence
468 from Aura MLS. *Geo. Research Letters.*, 33, L05709, doi: 10.1029/2005GL025505-2006.
- 469 Vogel, B., Günther, G., Müller, R., Grooß, J.-U., Hoor, P., Krämer, M., Müller, S., Zahn, A.,
470 and Riese, M.: Fast transport from Southeast Asia boundary layer sources to northern
471 Europe: rapid uplift in typhoons and eastward eddy shedding of the Asian monsoon
472 anticyclone, *Atmos. Chem. Phys.*, 14, 12745-12762, doi:10.5194/acp-14-12745-2014, 2014.



473

474 Waco, D. E.: Temperatures and turbulence at tropopause levels over hurricane Beula, Mon.

475 Weather Rev., 98, 749–755, 1970.

476 Wei, M. Y.: A new formulation of the exchange of mass and trace constituents between the

477 stratosphere and troposphere. Journal of Atmospheric Science., 44(20), 3079–3086,

478 doi:10.1175/1520-0469-1987.

479 Zhan, R. and Wang, Y.: Contribution of tropical cyclones to stratosphere–troposphere

480 exchange over the northwest Pacific: estimation based on AIRS satellite retrievals and

481 ERA-Interim data, J. Geophys. Res., 117, D12112, doi: 10.1029/2012.

482 Zou, X., and Y. Wu.: On the relationship between Total Ozone Mapping Spectrometer

483 (TOMS) ozone and hurricanes. J. Geophys. Res., 110, D06109, doi:

484 10.1029/2004JD005019-2005.

485

486

487

488

489

490

491

492

493

494

495

496

497 **Table:**

498 **Table 1.** Cyclone name, cyclone Intensity (CI), centre latitude, centre longitude, estimated
 499 central pressure and estimated cross-tropopause mass flux with respect to cyclone centre
 500 for C1 (NW side), C2 (NE side), C3 (SW side) and C4 (SE side), respectively.

501

Cyclone	CI	Centre Latitude	Centre Longitude	Estimated Central Pressure (hPa)	Flux @500km			
					C1	C2	C3	C4
03B	CS	23.5	66	986 (25Jun2007)	-0.013	0.661	-0.603	-0.258
Aila	SCS	22	88	968 (25May2009)	1.90E-04	0.191	-0.299	-0.072
Helen	SCS	16.1	82.7	990 (21Nov2013)	0.025	0.216	-0.095	-0.11
Jal	SCS	11	84	988(6Nov2010)	0.025	0.384	-0.4	-0.218
Laila	SCS	14.5	81	986 (19May2010)	-0.012	0.123	-0.352	-0.299
Mahasen	CS	18.5	88.5	990 (15May2013)	-0.006	0.354	-0.473	-0.256
Nilam	CS	11.5	81	990 (31Oct2012)	0.016	0.313	-0.274	-0.097
Nargis	VSCS	16	94	962 (2May2008)	-0.828	0.094	-1.946	0.384
Giri	VSCS	19.8	93.5	950 (22Oct2010)	-0.518	0.022	-0.823	0.032
Gonu	SuCS	20	64	920 (4Jun2007)	-0.502	0.123	-2.563	0.37
Lehar	VSCS	13.2	87.5	980 (26Nov2013)	-0.55	0.119	-2.019	0.411
Madi	VSCS	13.4	84.7	986 (10Dec2013)	-0.375	0.054	-1.449	0.352
Phailin	VSCS	18.1	85.7	940 (11Oct2013)	-0.9	0.179	-2.576	0.479
Phet	VSCS	18	60.5	964 (2Jun2010)	-1.058	0.203	-2.698	0.559
SIDR	VSCS	19.5	89	944 (15Nov2007)	-0.493	0.066	-0.926	0.231
Thane	VSCS	11.8	80.6	970 (29Dec2011)	-1.272	0.356	-2.979	0.558

502

503

504



505 **Figure captions:**

506 **Figure 1.** Tropical cyclone tracks of different categories (cyclonic storm (CS, blue color),
507 severe cyclonic storm (SCS, orange color), very severe cyclonic storm (VSCS, red color)
508 and super cyclonic storm (SuCs, magenta color)) that occurred over North Indian Ocean
509 during 2007 - 2013.

510 **Figure 2.** Cyclone centered – composite of mean difference in the tropopause parameters
511 between climatological mean (2007-2013) and individual tropopause parameters observed
512 during cyclones(irrespective of cyclone intensity) in (a) CPH (km), (b) LRH (km), (c) CPT
513 (K), (d) LRT (K), (e) COH (km) and (f) TTL thickness (km). Black circles are drawn to
514 show the 250 km, 500 km, 750 km and 1000 km away from cyclone center.

515 **Figure 3.** Normalized cyclone centered – composite of mean ozone mixing ratio observed
516 during cyclones(irrespective of cyclone intensity) at (a) 82hPa, (b) 100hPa, (c) 121hPa, (d)
517 146 hPa levels by MLS during 2007-2013. (e) to (h) same as (a) to (d) but for normalized
518 mean difference in the ozone mixing ratio between climatological mean (2007-2013) and
519 individual events. Black circles are drawn to show the 250 km, 500 km, 750 km and 1000
520 km away from cyclone center. Sectors showing C1 (NW), C2 (NE), C3 (SW) and C4 (SE)
521 are also shown in (a).

522 **Figure 4.** Same as Fig. 3, but for water vapor mixing ratio.

523 **Figure 5.** Cross-tropopause flux estimated in the (a) C1 (NW), (b) C2 (NE), (c) C3 (SW), and
524 (d) C4 (SE) sectors from the centre of cyclone for different cyclone intensities (estimated
525 based on cyclone centre pressure). Red lines show the best fit.

526 **Figure 6.** Schematic diagram showing the variability of CPH (brown color line) and COH
527 (magenta color line) with respect to the centre of cyclone. Spiral bands of convective
528 towers reaching as high as COH are shown with blue color lines. Light blue (red) color up



529 (down) side arrow shows the up drafts (downdrafts/subsidence). Thickness of the arrows
530 indicates the intensity.

531

532 **Table caption:**

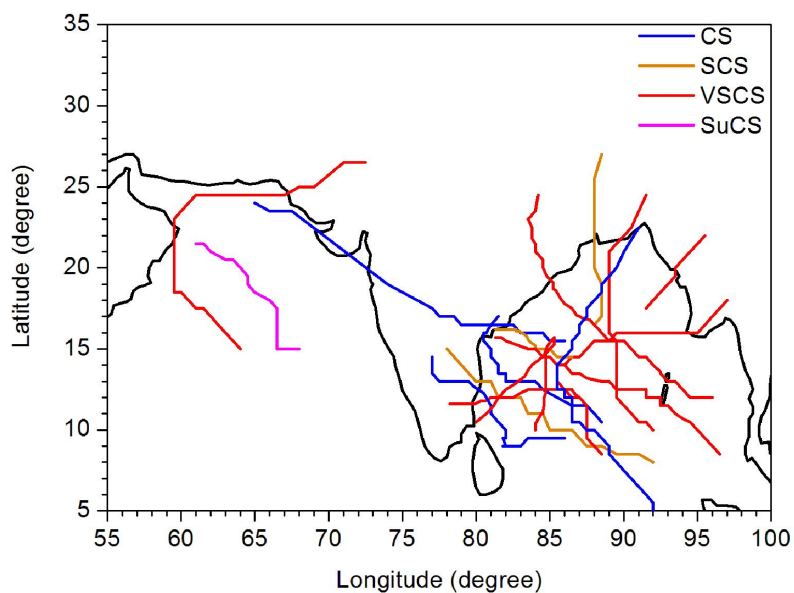
533 **Table 1.** Cyclone name, cyclone Intensity (CI), centre latitude, centre longitude, estimated
534 central pressure and estimated cross-tropopause mass flux with respect to cyclonecentre
535 for C1 (NW side), C2 (NE side), C3 (SW side) and C4 (SE side), respectively.

536



537 **Figures:**

538



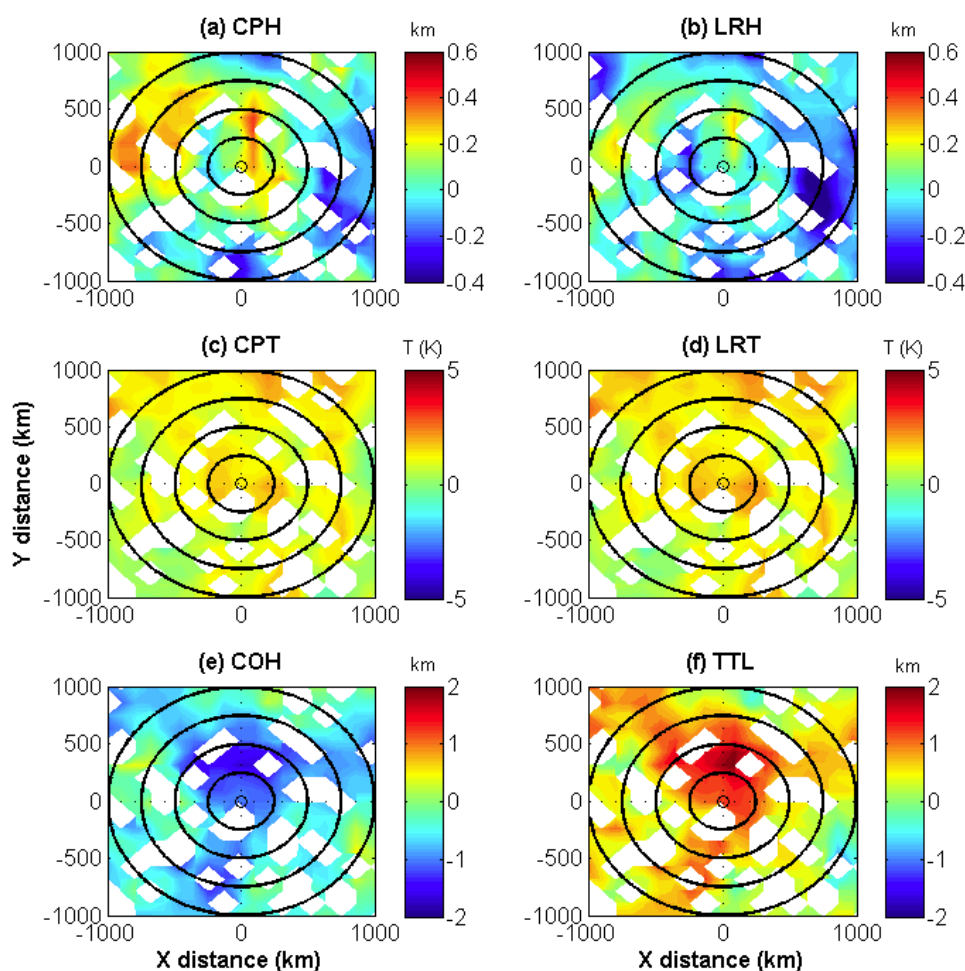
539

540 **Figure 1.** Tropical cyclone tracks of different categories (cyclonic storm (CS, blue color),

541 severe cyclonic storm (SCS, orange color), very severe cyclonic storm (VSCS, red color)

542 and super cyclonic storm (SuCs, magenta color)) that occurred over North Indian Ocean

543 during 2007 - 2013.

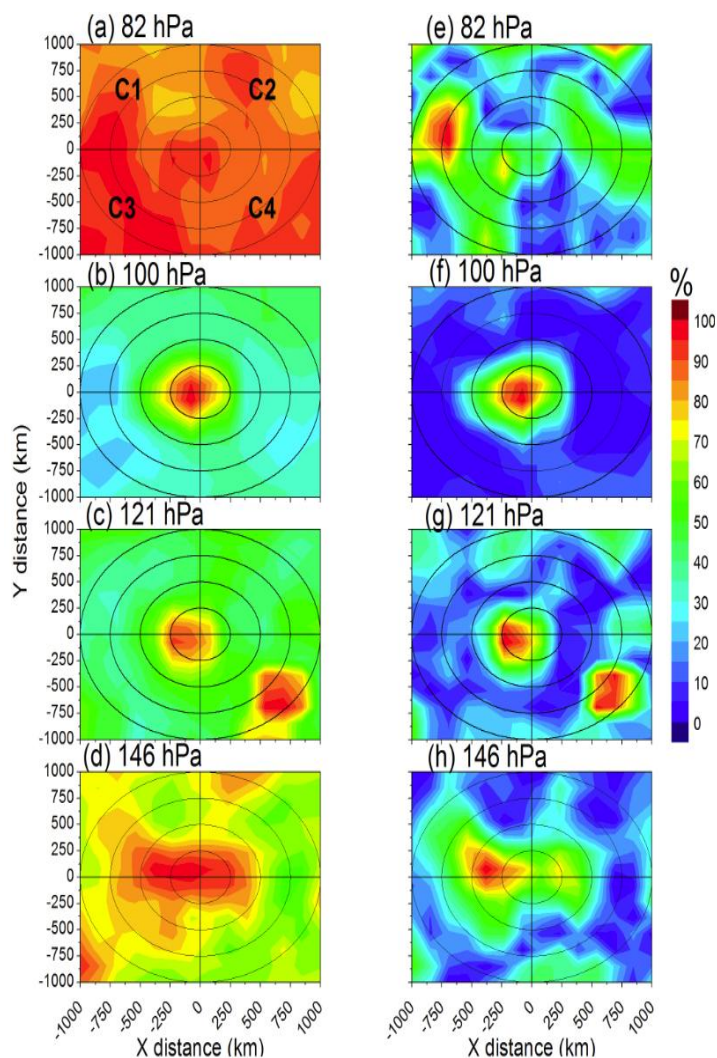


544

545 **Figure 2.** Cyclone centered – composite of mean difference in the tropopause parameters
546 between climatological mean (2007-2013) and individual tropopause parameters observed
547 during cyclones (irrespective of cyclone intensity) in (a) CPH (km), (b) LRH (km), (c) CPT
548 (K), (d) LRT (K), (e) COH (km) and (f) TTL thickness (km). Black circles are drawn to
549 show the 250 km, 500 km, 750 km and 1000 km away from cyclone center (taken from
550 Ravindra Babu et al., ACP, 2015).

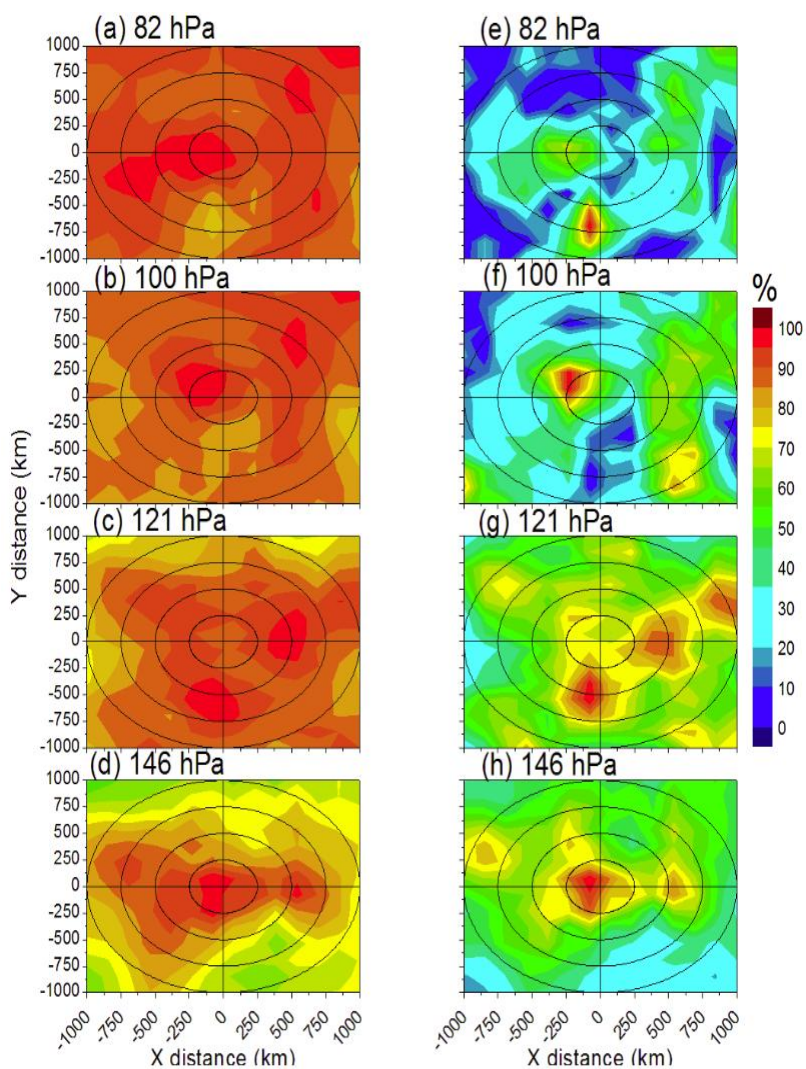
551

552



553

554 **Figure 3.** Normalized cyclone centered – composite of mean ozone mixing ratio observed
 555 during cyclones (irrespective of cyclone intensity) at (a) 82 hPa, (b) 100 hPa, (c) 121 hPa, (d)
 556 146 hPa levels by MLS during 2007-2013. (e) to (h) same as (a) to (d) but for normalized
 557 mean difference in the ozone mixing ratio between climatological mean (2007-2013) and
 558 individual events. Black circles are drawn to show the 250 km, 500 km, 750 km and 1000
 559 km away from cyclone center. Sectors showing C1 (NW), C2 (NE), C3 (SW) and C4 (SE)
 560 are also shown in (a).



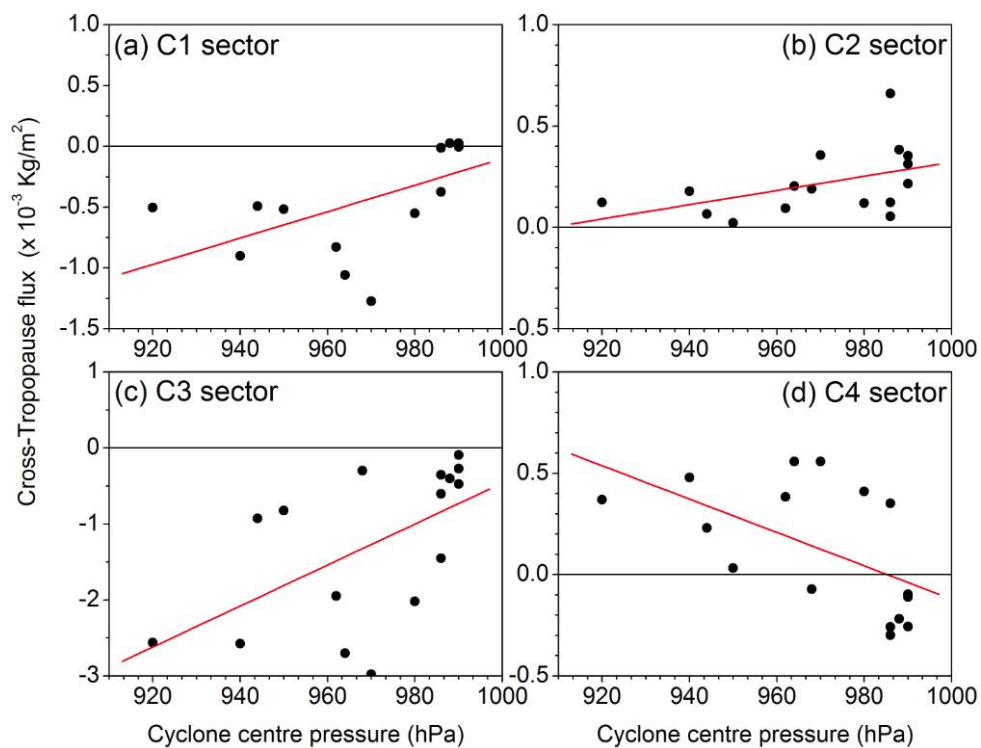
561

562 **Figure 4.** Same as Fig. 3, but for water vapor mixing ratio.

563



564



565

566 **Figure 5.** Cross-tropopause flux estimated in the (a) C1 (NW), (b) C2 (NE), (c) C3 (SW), and
567 (d) C4 (SE) sectors from the centre of cyclone for different cyclone intensities (estimated
568 based on cyclone centre pressure). Red lines show the best fit.

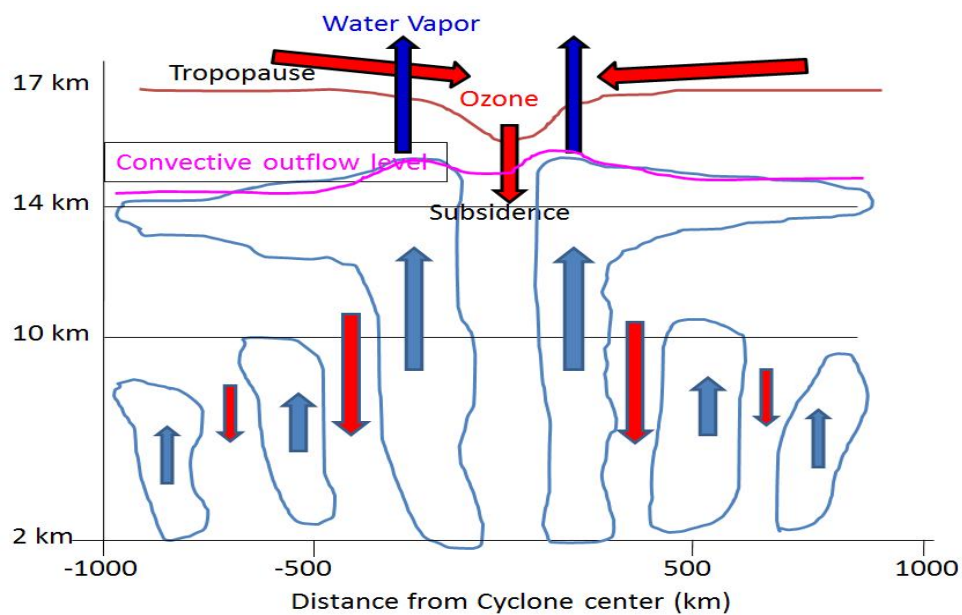
569

570

571

572

573



574

575 **Figure 6.** Schematic diagram showing the variability of CPH (brown color line) and COH
576 (magenta color line) with respect to the centre of cyclone. Spiral bands of convective
577 towers reaching as high as COH are shown with blue color lines. Light blue (red) color up
578 (down) side arrow shows the up drafts (downdrafts/subsidence). Thickness of the arrows
579 indicates the intensity.